Changes in the Structure of the Tropical Subcloud Layer from the Undisturbed to Disturbed States

K. L. ECHTERNACHT

Institute for Acoustical Research, Miami, Fla. 33130

M. GARSTANG

Department of Environmental Sciences, University of Virginia, Charlottesville 22903

(Manuscript received 21 June 1975, in revised form 24 November 1975)

ABSTRACT

Results of the analysis of measurements of temperature, mixing ratio, and horizontal wind speed are presented. The data were collected using a tethered ballon system during the 1969 BOMEX during periods of undisturbed and disturbed weather conditions. The results show that substantial changes occur in the character and stratification of the lower subcloud layer from the undisturbed to disturbed states. The lapse rate, height of the mixed layer, and estimated surface fluxes under disturbed conditions are to be obtained from the observations. These values are applied to currently suggested parametric relationships of the mixed layer under undisturbed conditions. Totally unrealistic values of vertical motion are obtained. It is concluded that convective cloud scale downdrafts driven by evaporation are extremely important in determining the budget of the mixed layer under disturbed conditions.

1. Introduction

Earlier workers (Malkus, 1958, and others) have used aircraft soundings to describe the structure of the lower boundary layer of the trade wind atmosphere. For the western ends of the tropical oceans these observations show a well mixed layer separated from cumulus cloud base by a frequently quite shallow transitional layer. In the mixed layer, moisture (mixing ratio) is found to be nearly constant with height and temperature decreases at the dry adiabatic rate. Neutral to slightly stable conditions existed in the transitional layer. In the cloud layer, temperature decreased moist adiabatically and mixing ratio shows a slight decrease up to the trade wind inversion base.

In this paper we wish to present a series of tethered balloon observations which suggest that the above picture is true only for fair or undisturbed weather conditions. By choosing a method to stratify our observations into categories of undisturbed and disturbed weather we can show that there are substantial changes in the structure of the layer below convective cloud base from the undisturbed to disturbed states. We believe further that we have evidence to show that this change in structure is forced from the cloud layer rather than from the surface. The cloud layer feedback leads to changes in the stability of the subcloud layer. These changes must have significant bearing upon the life cycle of convective clouds or convective systems. If these changes in the subcloud layer persist over long time periods or occupy large horizontal space relative to the convective systems then these effects must be considered if we are to understand the development, maintenance, and decay of convective ensembles.

2. The observations

The tethered balloon system, the Subcloud Instrument and Telemetry System (SITS), has been described previously by Garstang *et al.* (1971). The balloon measurements were obtained during the summer of 1969 on the island of Barbados at two sites: Husbands on the leeside of the island and East Point on the extreme upwind coast. Sondes measuring wind speed (cup anemometer), dry bulb temperature (thermistor), and humidity (hygristor) were flown in both profiling and constant level modes up to a height of 400 m. Convective cloud base was generally near 600 m. In order to examine changes in the structure of the oceanic subcloud layer the measurements from the upwind site are presented in this paper. The upwind site was located approximately 400 m from the edge of a 10 m cliff marking the eastern extremity of the island of Barbados. The terrain inland from the cliff is flat, featureless, and devoid of all but low (<2 m) vegetation. Rolling sugar cane fields lie inland, starting approximately 1 km from the site. With the prevailing easterly flow the point vertically below the balloon characteristically lay on an arc some 200 to 400 m inland from the site. Ulanski (1971) has shown that, above the surface, the site is representa-

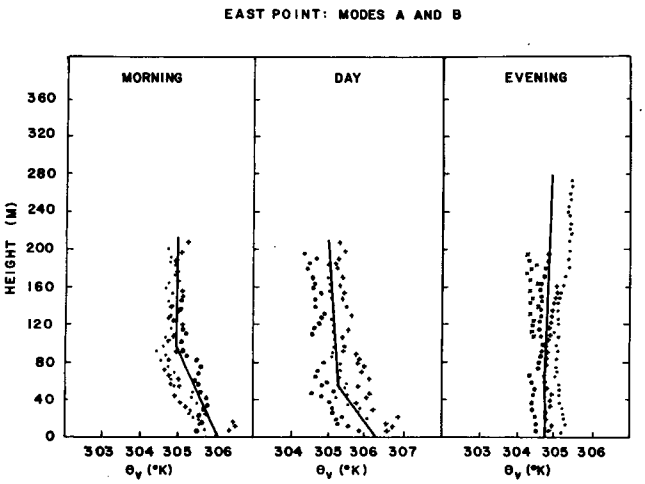

FIG. 1. Mean profile of θ_v—the undisturbed state.

tive of open ocean conditions. In that study analyses of wind and temperature data collected from multiple levels of a 16 m tower showed that the internal boundary separating sea—and land—influence flow was generally positioned between the 8 and 16 m levels of the tower. These results were substantiated in a later study which compared the 16 m level data with measurements collected from the buoy *Triton* (25 km upstream) and the *USCGS Discoverer* (100 km upstream) during the 1968 Barbados Experiment (Seguin, 1972). Our results (Figs. 1 and 2) do, however, suggest some land effects in the lowest 100 m under fair weather conditions.

Limited use is made of profiles obtained during the GATE International Sea Trials (GIST) conducted in August 1973 at an ocean station near 20°N and 60°W. A system developed by NOAA and the University of Wisconsin (Boundary Layer Instrumentation System, BLIS) was used. Five sondes were deployed at levels ranging from 100 to 1000 m. Sonde separation was either 200 or 300 m.

The above observations have been divided into five classes with each class representing a convective state of the atmosphere. The classification is based upon the percentage of raingage stations reporting rainfall on the island of Barbados. A similar classification was described by Simpson *et al.* (1967) and more recently defined, in some detail, by Garstang and Aspliden (1974). In this paper we will define each mode or class as follows:

Mode A Suppressed conditions—During this mode any process which contributes to the production of cloudiness and precipitation is inhibited.

Mode B Neutral—This mode favors the usual form of convection ranging from cumulus humilis to a few congestus and towering cumulus.

Mode C Weakly disturbed—This mode indicates the influence of conditions which actively produce cloudiness and precipitation such as a weak disturbance.

Mode D Moderately disturbed—The convection and rainfall are a direct result of a meso or small synoptic scale system.

Mode E Strongly disturbed—This mode is the result of the presence of a moderately large synoptic and/or mesoscale system.

Table 1 summarizes the foregoing in terms of the percentage of stations reporting rainfall.

In order to assess the stability of the subcloud layer during the different convective states the potential virtual temperature θ_v is used. Since the water vapor represents a large percentage of the energy transport through the subcloud layer, the use of θ_v takes into account the combined effect of temperature and water vapor on the stability of the lower atmosphere. The mean profiles of θ_v were computed from the profile data.

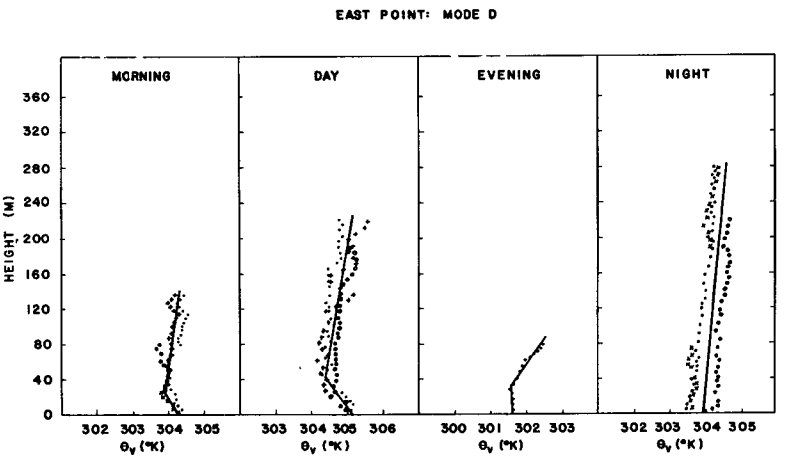

FIG. 2. Mean profile of θ_v—the moderately disturbed state.

TABLE 1. Modal classification.

Mode	Percentage of stations reporting rainfall
A	⩽15
B	16–55
C	56–75
D	76–85
E	⩾86

TABLE 2. The number of profiles for each time group and convective class.

Mode	Morning 0600–1000	Day 1000–1700	Evening 1700–2000	Night 2000–0600
A/B	6	7	7	
D	5	8	2	10
E	2	6	7	4

a. Mean profiles

A total of 64 separate profiles from the upwind site are used; 18 single sondeflights and 23 flights using two sondes separated by vertical distances of 30–150 m. Of the 64 profiles approximately 31% were obtained during undisturbed conditions and the remainder in disturbed weather. These two basic states are subdivided according to the above classes. Average lapse conditions representative of the different classes were obtained by averaging individual profiles over 5 m intervals from the surface (or lowest level) to the highest level. The θ_v was computed for each ascent and descent profile for each time and mode group using the individual profiles of temperature and mixing ratio. The average θ_v lapse was computed by fitting a least squares line to the individual profiles. Table 2 presents a breakdown by convective class of the number of soundings used for each mean profile.

The Mode A/B case, representative of undisturbed conditions, exhibits, during the day, instability in the lowest 40 m and neutral to slightly unstable through the remainder of the lower subcloud layer (Fig. 1). From aircraft measurements during BOMEX, Donelan and Miyake (1973) found that the neutral conditions extended to a height of approximately 500 m. Above this to the lower levels of the cloud layer conditions were stable.

During periods of moderately disturbed conditions, the Mode D case illustrated by Fig. 2, the instability, characteristic of the lower levels of the layer during the day, is much shallower compared to that observed during undisturbed periods. Above the shallow surface layer conditions are stable in contrast to the slightly unstable or neutral conditions of the undisturbed state. For strongly disturbed periods (Fig. 3) the stability extends throughout the lower subcloud layer to the surface. We will present evidence below that suggests that the increased stability, associated with increasing convective activity, is due directly to cloud layer/subcloud layer coupling.

3. Analysis of fixed-level observations

a. Analysis techniques

One limitation on the use of the SITS fixed level data is that the sonde did not incorporate explicit height determining sensors. As a consequence, the data include influences due to both the motions of the balloon and sonde. The motions of the balloon were studied using measurements taken both manually and automatically (Garstang *et al.*, 1971; Murday, 1970). The data were taken during undisturbed and weakly disturbed conditions. Murday (1970) found that during undisturbed conditions the fluctuations in height were small with periods of about 2 to 5 min showing the greatest variance (Fig. 4a). Elevated levels of variance in the spectra of mixing ratio and horizontal wind speed are shown in Fig. 4a for the higher frequencies. These do not coincide with fluc-

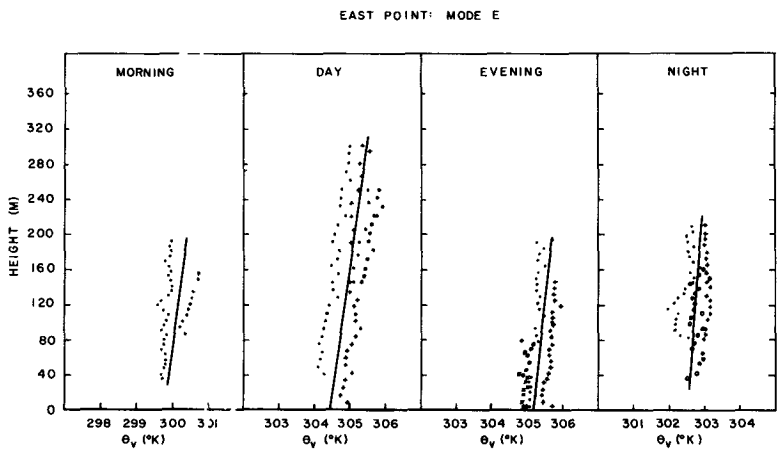

FIG. 3. Mean profile of θ_v—the strongly disturbed state.

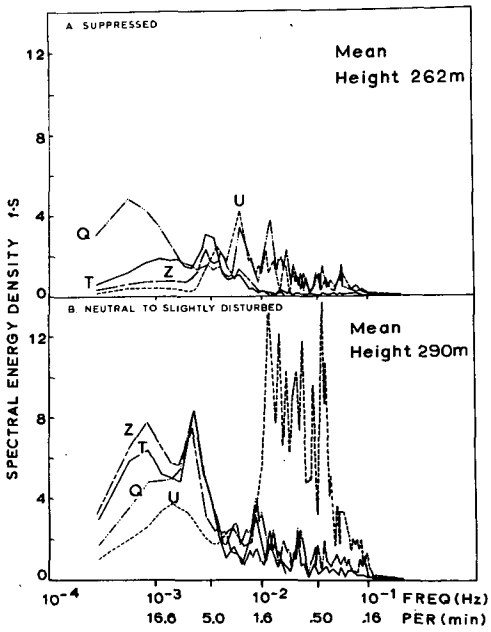

FIG. 4. The spectra of sonde measured temperature, moisture, and horizontal wind speed vs height change: A) suppressed state; B) neutral to slightly disturbed state. Units: fS_{zz}, $(m^2\ s^{-1})\times10^{-2}$; fS_{TT}, $(°C^2\ s^{-1})\times10^{-6}$; fS_{QQ}, $(g^2\ kg^{-2}\ s^{-1})\times10^{-6}$; fS_{uu}, $(m^2\ s^{-2})\times10^{-6}$.

tuations in height and probably reflect real changes in wind and water vapor.

For this study, motion data from a weakly disturbed case were compared with the results of Garstang *et al.* During periods of more active convection there exists a decided shift toward lower frequencies of the low frequency band in the spectra of height change, wind speed, humidity, and temperature (Fig. 4b). We believe that the large increase in the low frequency band reflects actual fluctuations in the atmospheric variables as well as vertical displacements of the balloon. These fluctuations with periods equal to and longer than 100 s probably reflect motions associated with convective clouds and convective cloud groups. The increase in variance in the high frequency band of the wind speed ($\geqslant 10^{-2}$ Hz) reflects both increased gustiness as well as spurious high frequency noise generated by the cup anemometer due to increased swinging and horizontal surging of the sonde. The surging results from changes in the catenary of the line and this effect is much more pronounced than the swinging of the sonde.

Despite the uncertainties associated with balloon and sonde motions, Figs. 4a and b do show a remarkable change in low frequency variance from suppressed to slightly disturbed conditions. We ascribe this increase in low frequency variance to convective cloud processes. Part of the analysis that follows concentrates upon the relative changes that are observed between the spectra of undisturbed and disturbed days. In such a comparison account can be taken of the fact that the sonde is not in fact fixed in space.

The time series of temperature, mixing ratio, and horizontal wind speed, from fixed-level observations, were transformed into frequency space by direct harmonic analysis using the fast Fourier transform (FFT) algorithm developed by Cooley and Tukey (1965). The spectral estimates were computed using the real valued Fourier coefficients returned by the algorithm. The resulting spectra are presented by convective class.

In this paper the spectra and cospectra of the fixed level data are presented as the product of the frequency f_n with the spectral estimates $S_{xx}(f)$ or cospectral estimates $S_{xy}(f)$ versus the frequency f_n. The spectra are plotted in log-log form. The abscissa f_n is the frequency f normalized by the fraction of the maximum wind:

$$f_n = f\cdot\left(\frac{U_z(i)}{U_{\max}}\right)^{-1}. \tag{1}$$

The normalized frequency was used to correct the apparent frequency shift between levels which occurs due to differences in wind speed. The normalization fraction, $U_z(i)/U_{\max}$, is the following:

$$\text{fraction} = \frac{\text{average wind at level } i\text{, for all days (mode } x)}{\text{average max wind, for all days (mode } x)}.$$

Because of difficulties encountered in maintaining anemometer calibration little confidence could be placed on the absolute values of wind speed. As such,

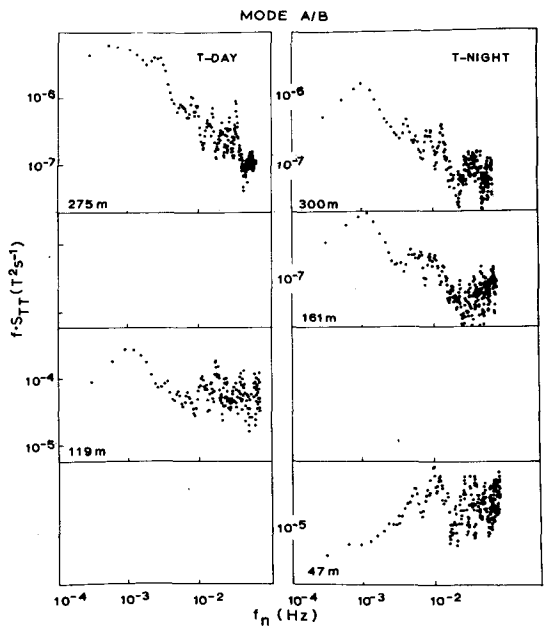

FIG. 5. Normalized temperature spectra—the undisturbed state: $fS_{TT}(T^2\ s^{-1})$ vs f_n.

averaged wind profiles were computed for each mode. The values of $U_z(i)$ and U_{max} were taken from the averaged profiles. Without the absolute value of wind speed it is not possible to determine exactly the spatial scale. Table 3 presents an approximate scale to be used with the spectra. This is based on mean wind speeds computed from BOMEX data (Ropelewski, 1975).

The degrees of freedom and the statistical confidence placed on the spectral estimates were not computed. As pointed out by Pond *et al.* (1971), the concept of degrees of freedom is nearly useless for atmospheric turbulence data. The actual scatter in the spectral estimates is used as a measure of the statistical variability.

b. *Temperature fluctuations*

For daytime undisturbed conditions (Fig. 5) the temperature spectra characteristically exhibit two distinct spectral peaks in the lower levels. The high frequency band ($f_n \geqslant 10^{-2}$) is indicative of the presence of small scale turbulent eddies of near surface origin while the low frequency peak ($f_n \leqslant 10^{-3}$) is thought to be due to larger scale organization of the flow as suggested by Grossman (1973) and DeSouza (1971).

TABLE 3. Approximate spatial scale.

f_n (Hz)	Spatial scale
10^{-4}–10^{-3}	10's km to 1 km
10^{-3}–10^{-2}	1 km to 100's m
$>10^{-2}$	<100's m

With increasing height through the mixed layer both the amplitude and variability of the small scale processes decrease while the spectral amplitude of the large scales increases with height.

These data suggest that the increased dominance with height of the low frequency fluctuations and the subsequent reduction in the higher frequencies is due, in part, to the organization of eddies of surface origin on increasingly larger scales and, as well, the presence of processes presumably of cloud layer origin in the upper layers.

During disturbed periods, conditions in the mixed layer are considerably changed. In comparing Figs. 6 and 7 with Fig. 5, it is evident that large scale processes determine the temperature structure through a greater depth of the mixed layer. This is particularly apparent in the lower levels. At the 144 m level the larger scales are dominant. The low frequency band ($10^{-3} < f_n < 10^{-2}$) corresponds to fluctuations with periods in the range of one to several minutes in duration. The reduced spectral variability and amplitude in the high frequency band ($f_n > 10^{-2}$) suggests a suppression of the small scale turbulent processes. Furthermore, for both the Mode D and E cases, the spectral

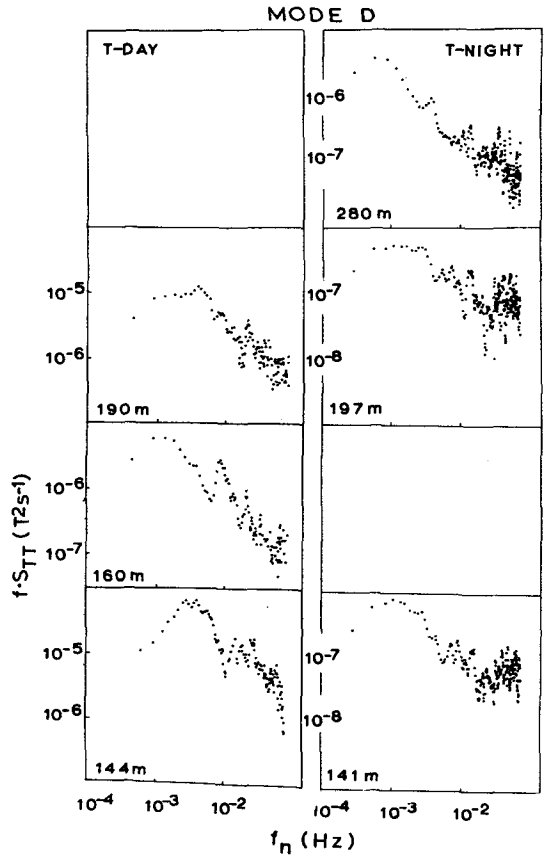

FIG. 6. Same as Fig. 5 except for the moderately disturbed state.

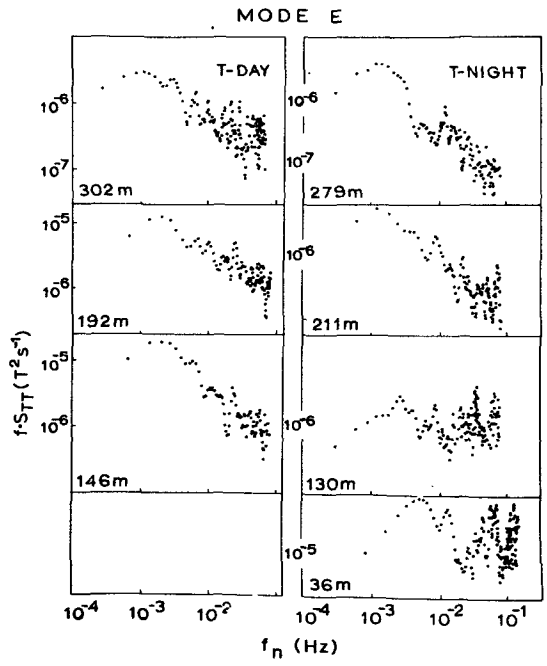

FIG. 7. Same as Fig. 5 except for the strongly disturbed state.

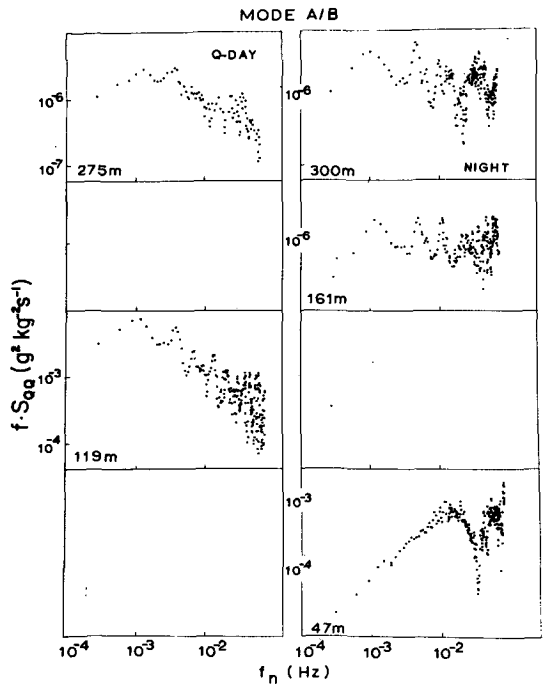

FIG. 8. Normalized mixing ratio spectra—the undisturbed state: fS_{QQ} ($g^2\,kg^{-2}\,s^{-1}$) vs f_n.

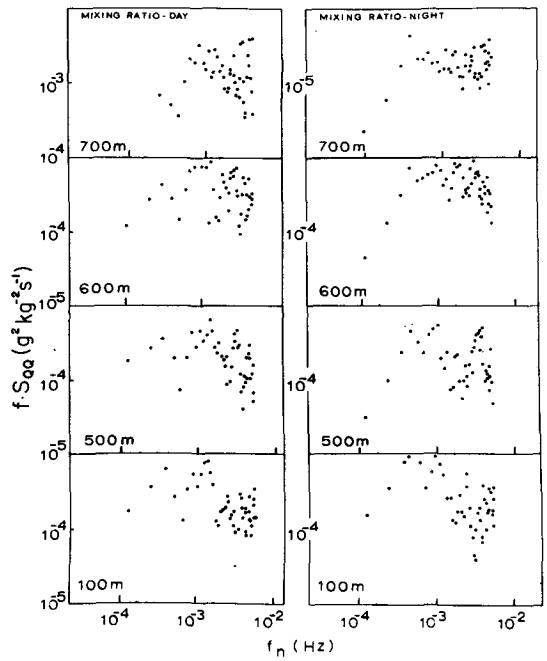

FIG. 9. Normalized mixing ratio spectra—(GIST measurements)—the undisturbed state. (Units as in Fig. 8).

distributions do not change significantly with height indicating a greater uniformity throughout the depth of the mixed layer.

In comparing the flux of sensible heat into the subcloud layer during disturbed vs undisturbed conditions, Seguin (1972) found that the flux from the sea surface was small at scales greater than the convective for the undisturbed state while during disturbed periods there was a large increase in sensible heat flux from both the ocean and cloud layer on the convective to synoptic scales. It was suggested that the shift to larger scales was due strictly to increased cloud layer/subcloud layer coupling on scales of the convective and larger. The fixed level spectra from this study confirm the increase in the amplitude of the convective scale as noted by previous studies. However, the foregoing picture is incomplete. It is the downward flux at the top of the mixed layer that is greatly enhanced and this is organized on a scale comparable to the convective flow due, directly, to the cloud layer/subcloud layer coupling. This conclusion is supported by the profile data. The enhanced downward flux of cloud layer air into the subcloud layer results in the observed stability. Thus, the observed scale shift in the surface flux is the result of the larger scale forcing together with the increased stability.

c. Moisture fluctuations

The spectra of mixing ratio exhibit differences between levels within the mixed layer but the strongest contrasts are between the undisturbed and disturbed states.

For undisturbed daytime conditions (Fig. 8) distinct spectral peaks are present at high and low wavenumbers but high frequency peaks are not as well

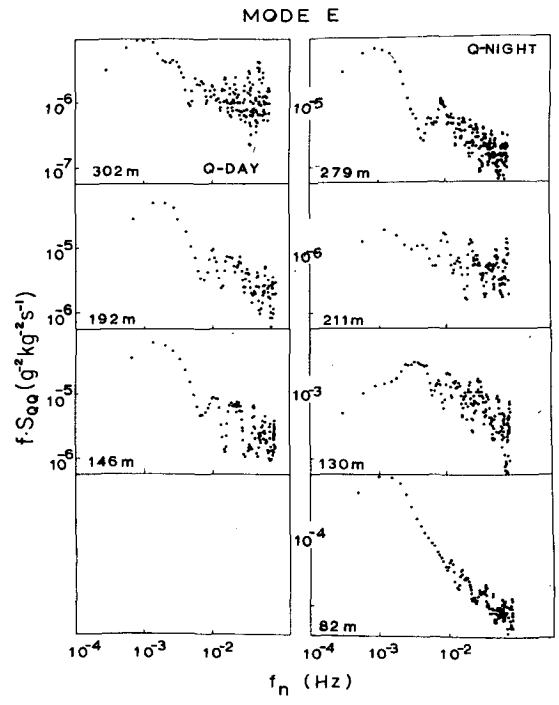

FIG. 10. Same as Fig. 8 except for the strongly disturbed state.

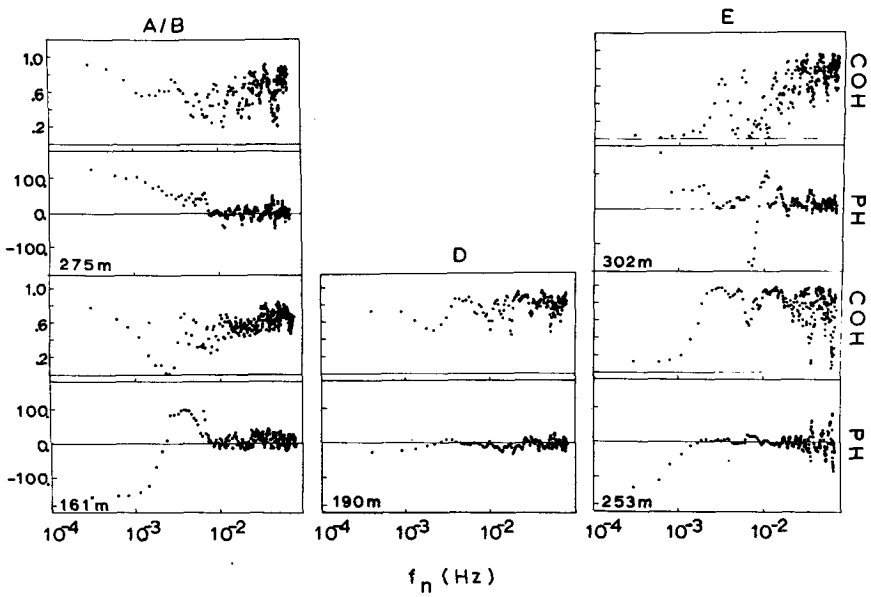

FIG. 11. Phase and coherence—temperature and mixing ratio—the undisturbed, moderately disturbed, and strongly disturbed states (day cases).

defined as in the temperature spectra. In the lower levels of the mixed layer the smaller scales exhibit a high degree of variability, but this variability decreases to a minimum with increasing height at the top of the mixed layer. As shown in previous studies (Bean *et al.*, 1972; Seguin, 1972), the smaller scale eddies are responsible for the bulk of the moisture transport in the lower levels but these are absorbed by the environment in the upper levels of the mixed layer. Above the mixed layer ($\geqslant 500$ m) the spectral amplitude associated with the convective scales ($f_n \sim 10^{-3}$) increases with height (Fig. 9) suggesting that the increased level of turbulence is associated with the influx of eddies of drier cloud layer air.

During disturbed periods, definite spectral bands are clearly distinguishable at high and low frequencies for both the day and night cases (Fig. 10). In contrast to the undisturbed case the total spectral energy is less in the mid and low levels of the mixed layer while the variability in the smaller scales increases with height throughout the mixed layer. This increase with height in the high frequency band was observed during undisturbed conditions, but only in the upper levels of the subcloud layer approaching cloud base (Figs. 8 and 9). It is suggested that the increased variability is evidence for the presence of a wide range of turbulent scales due directly to processes associated with penetrating downdrafts, including evaporation or detrainment of liquid water. The θ_v profiles for the disturbed cases (Figs. 2 and 3) are evidence for such penetration.

d. Phase and coherence of temperature and moisture fluctuations

Previous studies describing the details of the observed turbulent structure have shown that the vertical transports of sensible and latent heat are accomplished by buoyant eddies or plumes. Organization into cells and rolls can also occur on the kilometer scale. For the undisturbed case two general features of this eddy structure are exhibited by the phase and coherence estimates shown in Fig. 11.

1) The fluctuations of temperature and moisture are out of phase at larger scales and in phase at smaller wavelengths associated with buoyant eddies. The low frequency cutoff of the in phase signal is approximately 0.01 Hz at the 160 m level. This corresponds to a maximum plume diameter of the order of 500 m for a mean wind speed of 5.0 m s^{-1}. This result is consistent with the scale of thermals typically found in the tropical subcloud layer (Garstang *et al.*, 1971).

2) Malkus (1958) showed earlier that buoyant eddies rise to approximately the top of the mixed layer before losing buoyancy at normal rates of mixing. From this it might be concluded that eddies reaching the highest levels (i.e., most buoyant) must be warm and moist. In the present case the variability in coherence of the small scale fluctuations increases between the 160 and 275 m levels. Increased variability is the result of decreased parcel homogeneity. Such homogeneity appears to exist at the lower level but not at the upper level. Thus it would seem that mixing and entrainment must lead to increased variability at the higher level.

In contrast to the undisturbed case, during moderately disturbed periods (Fig. 11) the temperature and moisture are in phase over the entire wavenumber range. The coherence decreases somewhat at the lower frequencies, but, in general, is greater than 0.5. These

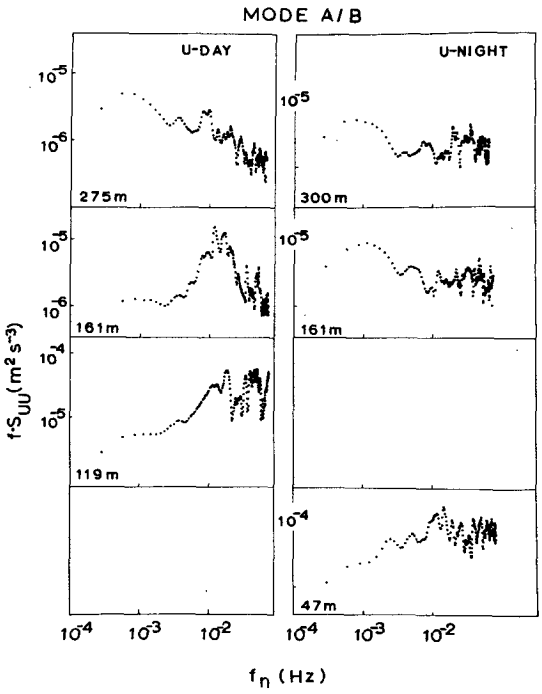

FIG. 12. Normalized wind speed spectra—the undisturbed state: $fS_{uu}(m^2 s^{-3})$ vs f_n.

results suggest the existence of eddies of increased scale with wavelengths of several hundreds of meters. Furthermore, the stable conditions present during disturbed weather (Figs. 2 and 3) suggest that these eddies are associated with downdrafts resulting from enhanced convection as postulated by Garstang and Betts (1974) and Echternacht (1973). For the Mode E case, the phase and coherence estimates suggest a return to undisturbed conditions. Mode E measurements were made following periods of intense convection. The drop in coherence in the lower frequencies may simply reflect the reduced convective activity present when the measurements were made.

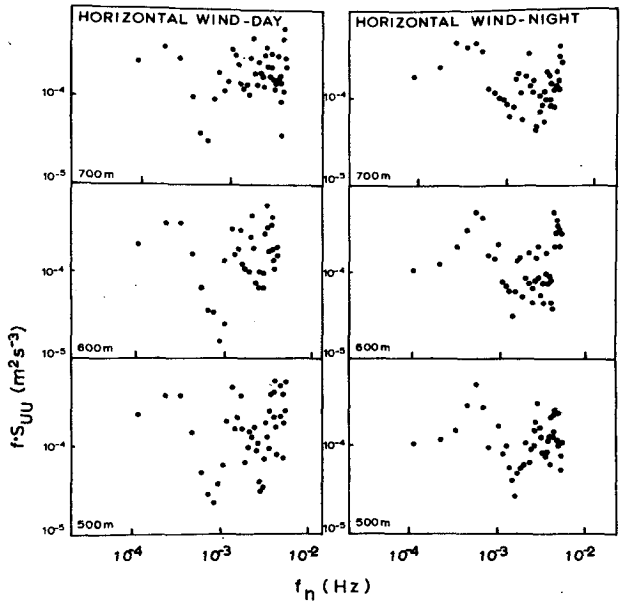

FIG. 13. Normalized wind speed spectra—(GIST measurements)—the undisturbed state. (Units as in Fig. 12).

e. Horizontal wind speed fluctuations

During undisturbed daytime periods the spectral energy in the lowest levels of the mixed layer is contained within a broad band of smaller scales with periods ranging from a few seconds to several minutes in duration (Fig. 12). Through the mid to upper levels of the mixed layer the spectral shift with height of the small scale band toward lower frequencies implies an increase in size with height of the momentum transport eddies. In the mid to upper levels the onset of the fall-off slope at large wavenumbers corresponds to scales which are two to three times larger than the distance from the surface suggesting that the momentum transport eddies are anisotropic at these levels. Increases in the level of variance and intermittency in the higher frequencies is restricted to the region between the top of the mixed layer and the lower levels of the cloud layer (Fig. 13). These findings show that during undisturbed periods the cloud layer/subcloud layer coupling is restricted to the upper

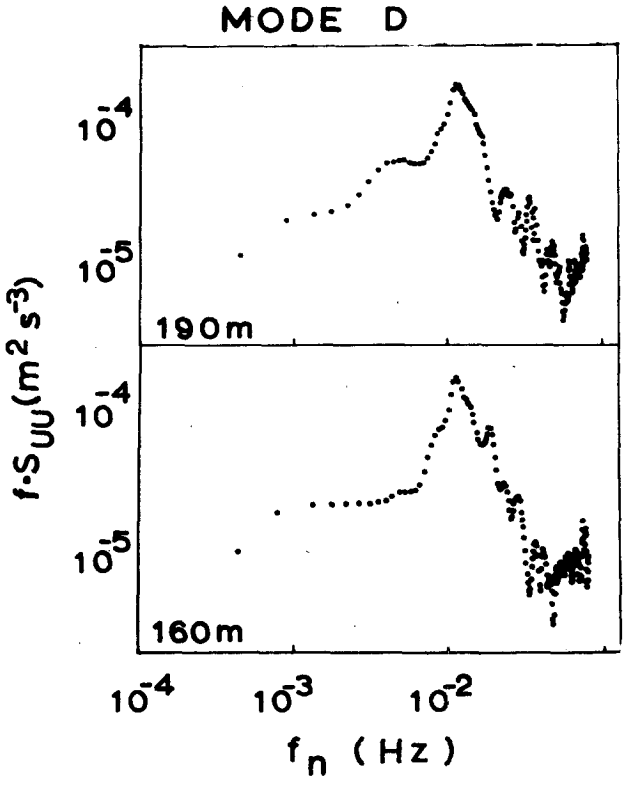

FIG. 14. Same as Fig. 12 except for the moderately disturbed state.

regions between the top of the mixed layer and cloud base.

The SITS balloon was flown in moderately disturbed conditions but not during the passage of intense storms. Consequently, the Mode E (strongly disturbed) data are representative of periods of reduced convective activity following the passage of a disturbance. These data are useful, however, in describing the effects of moderately large systems on the structure of the subcloud layer.

The spectra of wind speed for the disturbed cases show distinct differences compared to the undisturbed. During periods of active convection (Mode D shown in Fig. 14) the spectral amplitude in the 10^{-3}–10^{-2} Hz band (periods of ~8 to 1 min) is nearly an order of magnitude greater than for the undisturbed (Fig. 12). Although it is not possible to determine the absolute level of variance within the band, the relative increase between undisturbed and disturbed is significant. These data, supported by the temperature and humidity spectra and profiles, suggest that the increased band amplitude is the result of convective downdrafts. Following a disturbance during periods of reduced convection (Fig. 15) the 10^{-2} Hz peak is absent and larger scale processes are dominant. In an earlier study of a disturbance during the Line Islands Experiment, Zipser (1969) showed that the subcloud layer air was diluted by convective downdrafts. The data from this study suggest that after the passage of an intense storm the mixed layer is composed of air almost entirely of cloud layer origin and is stably stratified as shown by the stable lapse of θ_v (Fig. 3).

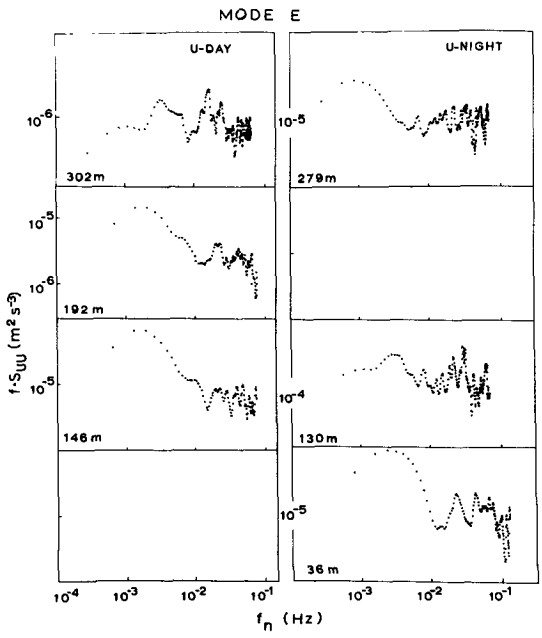

FIG. 15. Same as Fig. 12 except for the strongly disturbed state.

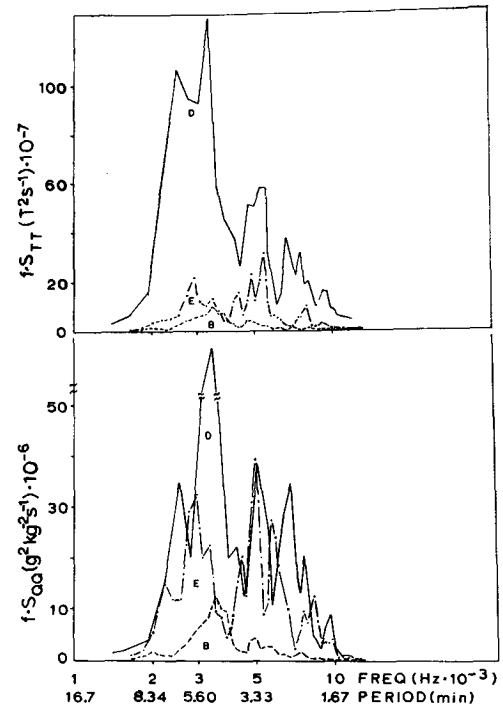

FIG. 16. Spectra for the convective scale passband: the undisturbed, moderately disturbed, and strongly disturbed states. Upper figure temperature; lower figure mixing ratio. Mode B (– – –), D (——), E (—·—).

4. The implications of cloud layer/subcloud layer coupling

In the previous sections it was shown that substantial changes in the structure of the subcloud layer occur with changing atmospheric state. The data suggest that during disturbed periods the convective scale process is the major factor contributing to the observed changes in subcloud layer structure. Spectra of temperature and mixing ratio from undisturbed and disturbed periods were examined for changes in the level of variance in a band of frequencies representative of convective scales.

Prior to spectral analysis, time series of fixed-level data (collected in the mid to upper levels of the mixed layer) were band-pass filtered. The residual signal contained frequencies in the range, $0.01 > f > 0.002$. The filtered spectra of temperature and mixing ratio are shown in Fig. 16. It can be seen that the level of variance in the pass-band increases by at least an order of magnitude from the neutral to the moderately disturbed state. The data suggest that the increased intensity is the result of convective scale mixing due directly to precipitation downdrafts and downdrafts associated with non-precipitating clouds. This increased mixing of cloud layer air into the mixed layer results in the observed change in mixed layer stability. As discussed in Section 3e, the low level of variance in the Mode E case is due to

the reduced convective activity at the time the measurements were made.

Present parameterization schemes do not adequately treat the subcloud layer under disturbed conditions. Existing models are concerned with the mixed layer during conditions of little or no cumulus activity (e.g., Deardorff, 1972; Tennekes, 1973; Carson, 1973) or assume that there exists a well-defined mixed layer even under disturbed conditions (Ogura and Cho, 1974). The data from this study indicate that pronounced changes occur in the subcloud layer when cumulus cloud convection is present.

Betts (1973a), among others, has proposed various methods to parameterize the thermal and moisture fluxes and the height of the mixed layer in the presence of non-precipitating cumulus. These processes are represented in terms of a mass flux or the equivalent compensating motion of the environment. The surface buoyancy flux is given by

$$(\overline{\theta_v' w'})_s = Q_e (lC_p)^{-1} [Q_s Q_e^{-1} + 0.08], \tag{2}$$

where Q_s and Q_e are the surface fluxes of sensible and latent heat and the equilibrium solution for the height h, of the mixed layer is the following.

$$h = \frac{1.2(\overline{\theta_v' w'})_s}{\gamma_v(-\hat{w})}. \tag{3}$$

$\gamma_v = \partial\theta_v/\partial z$ is the cloud layer stratification and $\hat{w}$ is the between cloud vertical velocity representing the sum of the mean vertical motion and a compensating subsidence between the clouds. The constant 1.2 is obtained from a relationship between the surface flux and the downward flux at the top of the mixed layer (subscript i):

$$(\overline{\theta_v' w'})_i = -0.2(\overline{\theta_v' w'})_s. \tag{4}$$

Betts (1973a) assumed this relationship held in the presence of cumulus. The coefficient 0.2 has been used by several authors, and has been confirmed for dry convection by a numerical study (Deardorff, 1974).

From an analysis of a disturbed BOMEX period Nitta and Esbensen (1974) determined the total between cloud subsidence $\hat{w}$ at mixed layer height to be -3.8 cm s^{-1}. The mixed layer height, h, moreover, was assumed to be stationary at 400 m. The results obtained are, however, critically dependent upon the choice of the depth of the mixed layer.

The observations from this study show that during disturbed periods a mixed layer height of 400 m is unrealistic. For these conditions (as shown in Fig. 2) the mixed layer height is approximately 40 m and the stratification $\gamma_v = 3.9 \times 10^{-5}$ K cm^{-1}. The surface flux is assumed to be $(\overline{\theta_v' w'})_s = 4.52$ K cm s^{-1}. We base our surface flux estimate upon Ulanski *et al.* (1973) and Garstang (1967). Ulanski *et al.* found that instantaneous fluxes can increase by an order of magnitude in the presence of downdrafts. Garstang showed an increase in fluxes of an order of magnitude in sensible heat and a factor of two in latent heat for disturbed cases. For undisturbed conditions Holland and Rasmussen (1973) obtain a value for the surface flux of about 2.26 K cm s^{-1}. A twofold increase in the average flux is therefore likely to be an underestimate. However, assuming such an increase we can compute the subsidence necessary to maintain a mixed layer height of 40 m. Under these circumstances Eq. (3) yields $-\hat{w} = 35$ cm s^{-1}. This is clearly an unrealistic value. With $h = 40$ m Nitta and Esbensen would probably obtain totally unrealistic vertical motions.

We must conclude that Eq. (3) cannot be applied in disturbed conditions. Eq. (3) is based on a balance between the heating rate *in* the mixed layer (suffix, m) and the heating rate *above* the mixed layer, namely

$$\frac{d\theta_{vm}}{dt} = \frac{1.2(\overline{\theta_v' w'})_s}{h} = -\hat{w}\gamma_v. \tag{5}$$

In subsequent work, Betts (1975) shows that cumulus convection *cannot* be parameterized solely in terms of a mass flux or the equivalent compensating motion of the environment. Instead both subsidence in terms of a between-cloud vertical motion and detrained heat and liquid water must be taken into account. In Betts' analysis the detrainment is a cooling term (dominated by evaporation) of opposite sign to the subsidence and typically a third of the magnitude. This process is therefore not negligible. Further, Betts (1973b) showed that in disturbed conditions downdrafts driven by evaporating precipitation cannot be neglected in the budget of the subcloud layer. The parameterization of the disturbed case must clearly include these effects to obtain more realistic results.

5. Conclusions

The data presented in this study show that substantial charges occur in the structure of the lower subcloud layer between undisturbed and disturbed weather conditions. As shown from the θ_v profiles, the undisturbed subcloud layer is characterized by an unstable lapse in the lowest levels and slightly unstable to neutral conditions above this to the transitional layer. With increased convective activity the mixed layer height is depressed downward and the lower subcloud layer exhibits a stable stratification due to the increased downward motion of air of cloud layer origin driven by evaporation.

The above is supported by the spectral analyses of fixed-level measurements. During disturbed conditions the larger convective size scales dominate the temperature spectra and the temperature and moisture

are in phase over the entire wavenumber range. The convective band-pass spectra of temperature and moisture show that the spectral levels increase by an order of magnitude during periods of enhanced convection. These results show that the observed change in subcloud layer structure is forced, not from the surface, but from the cloud layer in the form of convective downdrafts.

Under disturbed conditions the mixed layer model (Eq. 3) is unsuitable to explain the observed shallow mixed layer. It is clear that downdraft and evaporation processes driven from the cloud layer are extremely important to the budget of the mixed layer.

If these changes in subcloud layer structure persist over long time periods or occupy large horizontal space relative to the cloud systems then these effects must be understood if we are to understand the development, maintenance, and decay of convective ensembles and predict the surface fluxes.

Acknowledgments. The authors would like to thank Drs. Carl Aspliden, Ward Seguin, and Alan Betts for the many helpful discussions during the course of this work. The support of this work under a grant (# GA31601) from the National Science Foundation is gratefully acknowledged. The Institute for Acoustical Research provided support during the preparation stages of the manuscript.

REFERENCES

Bean, B. R., R. Gilmer, R. L. Grossman, R. McGavin and C. Travis, 1972: An analysis of airborne measurements of vertical water vapor flux during BOMEX. *J. Atmos. Sci.*, **29**, 860–869.

Betts, A. K., 1973a: Non-precipitating cumulus convection and its parameterization. *Quart. J. Roy. Meteor. Soc.*, **99**, 178–196.

——, 1973b: A composite mesoscale cumulonimbus budget. *J. Atmos. Sci.*, **30**, 597–610.

——, 1975: Parametric interpretation of trade-wind cumulus budget studies. *J. Atmos. Sci.*, **32**, 1934–1945.

Carson, D. J., 1973: The development of a dry inversion-capped convectively unstable boundary layer. *Quart. J. Roy. Meteor. Soc.*, **99**, 450–467.

Cooley, J. W., and J. W. Tukey, 1965: An algorithm for the machine calculation of complex Fourier series. *Math. Comp.*, **19**, 297–301.

Deardorff, J. W., 1972: Numerical investigation of neutral and unstable planetary boundary layers. *J. Atmos. Sci.*, **29**, 91–115.

——, 1974: Three dimensional study of the height and mean structure of a heated planetary boundary layer. *Bound. Layer Meteor.*, **7**, 81–106.

DeSouza, R. L., 1971: A study of the atmospheric flow over a tropical island. Ph.D. dissertation, Dept. of Meteorology, Florida State University, 230 pp.

Donelan, M., and M. Miyake, 1973: Spectra and fluxes in the boundary layer of the trade-wind zone. *J. Atmos. Sci.*, **30**, 444–464.

Echternacht, K. L., 1973: Investigations of the turbulent structure of the tropical subcloud layer. *Bull. Amer. Meteor. Soc.*, **54**, 165.

Garstang, M., 1967: Sensible and latent heat exchange in low latitude synoptic scale systems. *Tellus*, **3**, 492–508.

——, and C. I. Aspliden, 1974: Convective Cloud Code Manual. (Compiled for use during the GATE International Experiment).

——, and A. K. Betts, 1974: A review of the tropical boundary layer and cumulus convection: structure, parameterization, and modeling. *Bull. Amer. Meteor. Soc.*, **55**, 1195–1205.

——, M. Murday, W. R. Seguin, J. D. Brown and N. E. LaSeur, 1971: Fluctuations in humidity, temperature, and horizontal wind speed as measured by a subcloud tethered-balloon system. *Trans. IEEE Geophys. Elec.*, GE-9, 199–208.

Grossman, R. L., 1973: An aircraft investigation of turbulence in the lower layers of a marine boundary layer. Ph.D. dissertation, Dept. of Meteorology, Colorado State University, 166 pp.

Holland, J. Z., and E. M. Rasmussen, 1973: Measurements of the atmospheric mass, energy, and momentum budgets over a 500-kilometer square of tropical ocean. *Mon. Wea. Rev.*, **101**, 44–55.

Malkus, J. S., 1958: On the structure of the trade wind moist layer. Papers in Phys. Oceanog. and Meteor., Mass. Inst. of Tech. and Woods Hole Oceanog. Inst., Cambridge and Woods Hole, Mass., **13**, 47 pp.

Murday, M., 1970: High-frequency fluctuations of humidity temperature and horizontal wind from a sub-cloud tethered-balloon telemetry system. M.S. thesis, Dept. of Oceanography, Florida State University, 160 pp.

Nitta, T., and S. Esbensen, 1974: Heat and moisture budget analysis using BOMEX data. *Mon. Wea. Rev.*, **102**, 17–28.

Ogura, Y., and H. R. Cho, 1974: On the interaction between the subcloud and cloud layers in tropical regions. *J. Atmos. Sci.*, **31**, 1850–1859.

Pond, S., G. T. Phelps, J. Pacquin, G. McBean and R. W. Stewart, 1971: Measurements of the turbulent fluxes of momentum, moisture and sensible heat over the ocean. *J. Atmos. Sci.*, **28**, 901–917.

Ropelewski, C. F., 1975: BOMEX wind spectra derived from the boundary layer instrument package (BLIP). NOAA Tech. Rept. EDS BOMAP—17, 15 pp.

Sequin, W. R., 1972: A study of the tropical oceanic subcloud layer. Ph.D. dissertation, Dept. of Meteorology, Florida State University, 221 pp.

Simpson, J., M. Garstang, E. J. Zipser and G. A. Dean, 1967: A study of a non-deepening tropical disturbance. *J. Appl. Meteor.*, **6**, 237–254.

Tennekes, H., 1973: A model for the dynamics of the inversion above a convective boundary layer. *J. Atmos. Sci.*, **30**, 558–567.

Ulanski, S. L., 1971: A kinematic and thermodynamic description of the Prandtl layer circulation over Barbados. M.S. thesis, Dept. of Oceanography, Florida State University, 218 pp.

——, R. K. Hadlock and M. Garstang, 1973: The role of convection in surface property and velocity fluctuations. *Bound.-Layer Meteor.*, **6**, 183–195.

Zipser, E. J., 1969: The role of organized unsaturated convective downdrafts in the structure and rapid decay of an equatorial disturbance. *J. Appl. Meteor.*, **8**, 799–814.